

# Optical Response of Magnetically Actuated Biocompatible Membranes

## SUPPLEMENTARY INFORMATION 1

H. Joisten<sup>1,3</sup>, A. Truong<sup>1</sup>, S. Ponomareva<sup>1</sup>, C. Naud<sup>1</sup>, R. Morel<sup>1</sup>, Y. Hou<sup>2</sup>, I. Joumard<sup>1</sup>, S. Auffret<sup>1</sup>, P. Sabon<sup>1</sup>, B. Dieny<sup>1</sup>

1. Univ. Grenoble Alpes, CEA, CNRS, IRIG-SPINTEC, 38000 Grenoble, France

2. Univ. Grenoble Alpes, CEA, CNRS, IRIG-SYMMES, 38000 Grenoble, France

3. Univ. Grenoble Alpes, CEA, LETI, 38000 Grenoble, France

Corresponding Author's e-mail address: [helene.joisten@cea.fr](mailto:helene.joisten@cea.fr)

### Experimental method: Technological process for material preparation

#### Fabrication process of magneto-elastic membranes

The fabrication process developed at SPINTEC involves two major steps. The deep reactive ion etching technique (DRIE) seemed to be an attractive way to produce suspended and ready-to-be-actuated membranes in a systematic and highly reproducible manner. The first step in the process consists in embedding arrays of magnetic cylinders in a PDMS matrix. The second step is the most time consuming since the parts of the wafer that support the magnetic pillars have to be completely etched away from the backside in order to obtain suspended magnetically actuable membranes. Optimizing the parameters of the DRIE is a relatively challenging task. For this process, the Si wafers must have both of their sides polished, since UV lithography needs to be done on each side.

#### Level 1: Arrays of magnetic pillars

The arrays of magnetic pillars are arranged so that a 4" Si wafer can support many membranes. The permalloy pillars are grown by electrochemical deposition (ECD) on an Au layer, using a resist mould. The Au layer (100 nm) covers the whole area of the wafer. Then the resist AR 4400, which is particularly adapted for ECD, is spin-coated on the Au layer (5  $\mu\text{m}$ ). This is followed by a UV lithography step on the resist, which will serve as a 'mould' for the ECD. Once the pillars are grown, the resist AR 4400 is stripped away using an O<sub>2</sub> plasma etch. Indeed, once the resist AR 4400 is cured/baked, it becomes relatively hard to remove with acetone. The mask includes two levels. The first level is intended for the magnetic pillars, which are organized in two ways: in a hexagonal lattice and in a square lattice. Their diameters range from 1  $\mu\text{m}$  to 2  $\mu\text{m}$ . Both square and hexagonal arrangements either have particles with the same diameters or with different diameters. The second level of the mask allows us to produce circular membranes.

#### Level 2: Fabricating the suspended membranes

Once the magnetic pillars are grown, the whole surface of the wafer is covered with PDMS (about 5  $\mu\text{m}$ ). The wafer is then flipped over and a second UV lithography step is performed, using the second level of the mask. Regarding the mask alignments, a double mask aligner could be used in order to align mask levels that are on different sides of the wafer. In our case, the circular patterns in the second level were intentionally made to have smaller dimensions than the square patterns in the first level, so that a rough alignment can be sufficient. The choice of the photosensitive resist for this

step is crucial. The resist has to be negative in order to be compatible with our mask design and thick enough to endure the deep etching process. So far, several attempts have been made and the most successful results were obtained with the SU 8 resist masks.

The thicker the resist, the more difficult it becomes to work with and complications can occur during the soft baking. The DRIE process developed here is similar to the well-known Bosch process, except that a flow of  $O_2$  is added to the plasma. The Bosch process is well adapted for etching large thicknesses of silicon while keeping the sidewalls as vertical as possible. First, a  $C_4F_8$  plasma is applied to produce  $CF_n$  polymers that will passivate the surface of the resist and the sidewalls. Then the Si etching occurs in two steps, using a mix of  $SF_6 + O_2$ . During the passivation step, a layer of  $CF_n$  polymers forms on the Si surface that we want to etch. For that reason, a magnetic field is activated in the main chamber of the DRIE machine in order to favour the bombardment (physical etching) of that polymer layer for a very short amount of time. This step is called the 'boost' step. Once the Si in the trenches is exposed, the magnetic field is removed in order to favour the chemical etching of Si by  $F^+$  ions. These passivation and etching steps are repeated in a cyclic manner for as long as necessary to dig through the entire thickness of the wafer, each step lasting a few seconds. The original Bosch process does not mention the use of  $O_2$ . One of the issues of relying only on  $SF_6$  to etch Si is that  $SF_6$ , after it is decomposed into  $SF_5^-$  and  $F^+$ , tends to be regenerated through the recombination of  $SF_5^-$  and  $F^+$  ions. Since the  $F^+$  ions are the species that are essential to the etching of silicon, the purpose of adding  $O_2$  in our case is to prevent both ions from recombining. However,  $O_2$  plasmas tend to react with the resist mask, which accelerates its deterioration, knowing that the 'boost' step already contributes to its deterioration. As a result, the addition of  $O_2$  should be done carefully by adjusting the flow. The sample's temperature can also be controlled, especially to prevent the resist mask from burning.

Alternatively, instead of a resist mask, a metal mask made of a thin layer of Al can be considered. However, when they are bombarded by ions, Al layers tend to produce tiny metallic particles that can fall in the trenches and cover a part of the area that we want to etch.

The process for obtaining magneto-elastic membranes with the DRIE technique still requires some adjustments in order to yield better results. In Fig. 1(c), one can see an example of a silicon wafer obtained after the DRIE. Etching is not uniform, since some regions are still filled with Si while for other regions the membranes are perfectly suspended. Such inhomogeneity in the DRIE process is assumed to be due to an inhomogeneous thermal exchange between the wafer and the supporting plate during the etching. In order to make the thermal exchange more uniform, a special type of glue may be used to stick the wafer on the supporting plate. However, since we want the membranes to be intact after the process, no glue was used. Moreover, it also seems difficult to remove the Au layer in a proper manner, without risking to destroy the membranes.

The influence of the presence of an Au layer on the overall mechanical properties of the suspended membranes has been investigated. Despite the fact that the obtained result is not optimal for the moment, some suspended membranes have successfully been obtained and optically tested.

# Optical Response of Magnetically Actuated Biocompatible Membranes

## SUPPLEMENTARY INFORMATION 2

H. Joisten<sup>1,3</sup>, A. Truong<sup>1</sup>, S. Ponomareva<sup>1</sup>, C. Naud<sup>1</sup>, R. Morel<sup>1</sup>, Y. Hou<sup>2</sup>, I. Joumard<sup>1</sup>, S. Auffret<sup>1</sup>, P. Sabon<sup>1</sup>, B. Dieny<sup>1</sup>

1. Univ. Grenoble Alpes, CEA, CNRS, IRIG-SPINTEC, 38000 Grenoble, France
2. Univ. Grenoble Alpes, CEA, CNRS, IRIG-SYMMES, 38000 Grenoble, France
3. Univ. Grenoble Alpes, CEA, LETI, 38000 Grenoble, France

Corresponding Author's e-mail address: [helene.joisten@cea.fr](mailto:helene.joisten@cea.fr)

### Complement on Magnetic field B

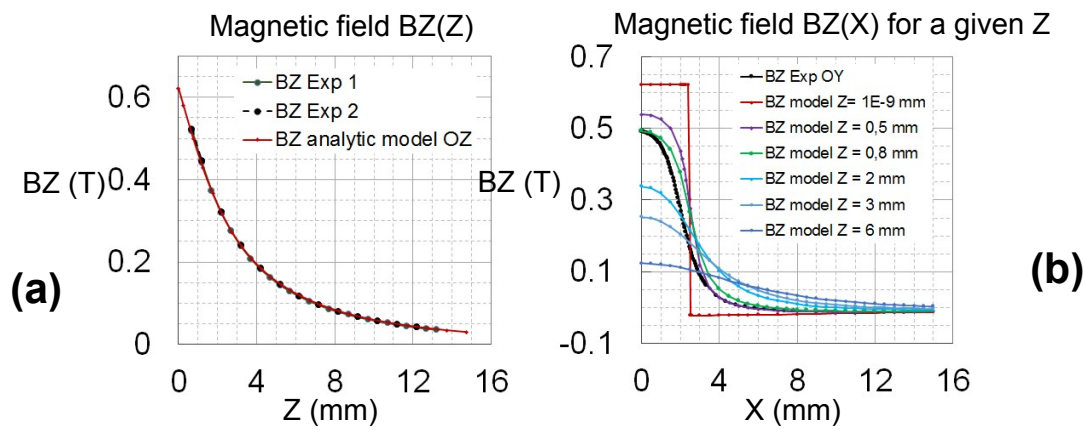


**Figure S1.** Experimental and modelled magnetic field  $B_z$ , as a function of  $Z$ , and  $X$ , generated by the NdFeB magnet,  $\mu_0 M_s = 1,29$  T,  $20$  mm  $\times$   $20$  mm  $\times$   $5$  mm; along OZ and OX axis (both horizontal). OY axis being vertical;  $(0,0,0)$  centered on the magnet face. Analytic model of “two charged surfaces”  $B_z(X,Y,Z) = B_{z1} - B_{z2}$ , according to Eq.3. **(a)**  $B_z = f(Z)$  in air, along OZ axis  $(X,Y) = (0,0)$ , **(b)**  $B_z = f(X)$  in air, along a transverse OX axis  $(Y=0)$ , for various given  $Z$ . Experimental curves/ dots in black color.

See in the paper, the magnetic field expression, given by:

$$B_z(X,0,Z) = [b_z(X,0,Z) - b_z(X,0,(Z+h))]$$

where

$$b_z(X,0,Z) = \left( \frac{\mu_0 M_{MAG}}{4\pi} \right) \cdot 2 \cdot \left[ \tanh^{-1} \left( \frac{(X+a) \cdot b}{Z \cdot (\sqrt{(X+a)^2 + b^2 + Z^2})} \right) - \tanh^{-1} \left( \frac{(X-a) \cdot b}{Z \cdot (\sqrt{(X-a)^2 + b^2 + Z^2})} \right) \right] \quad (3)$$

The model fits perfectly with the field  $B_z(Z)$  measured by an Hall sensor, as shown in Fig.S1(a).

In Fig.S1(b), are shown experimental (black color) and modelled  $B_z(x)$  curves, measured and modelled along OX-axis, perpendicularly to OZ-axis, for various given  $Z$ ,  $(Y=0)$ . The modelled curves are displayed in various colors, each ones for a given  $Z$ . Finally, the superimposed experimental curve, in black color, corresponds to the  $Z \sim 0.8$  mm model for small  $X$  values, and corresponds to the  $Z \sim 0.5$  mm model for larger  $X$  values.

The fact that the experimental curve  $B_z(X)$ , slightly slides from  $Z = 0.8$  to  $0.5$  mm models, is likely due to a tiny deviation of the Hall sensor course along  $OX$  axis during experiment. The expression in **Eq.(3)** is therefore reliable for expressing the magnetic field  $B_z(X,0,Z)$ , applied on magnetic pillars embedded in membranes.

**Average magnetic field  $BZ = BZ(X)$  along  $OX$**

See **Fig.S1** and in the paper **Fig.4**.

$B_z$  is assumed to be constant,  $B_z(X,Y,Z) = B_z(0,0,Z)$ , on the hatched surface  $S_{red}$ , and  $B_z(X,Y,Z) = 0$  on the yellow color periphery;  $S_{red}$  is smaller than the membrane surface  $S_m = \pi R_m^2$ ;  $2 \times w_x \approx 5.5$  mm, leading to  $S_{red} \sim 80\%$  of the membrane surface  $S_m$  (See  $S_{red}$  expression in the text).

This approximation using the reduced surface  $S_{red}$  for considering a constant  $BZ$ , is in particular well suited for the magnet positioned at around  $Z = 4$  mm, as shown in the **Table1** below. For larger  $Z$  such as  $4 < Z < 6$  mm, the difference between the average field  $BZ$  and the approximate  $BZ$  slightly increases, remaining below 10%.

X (mm)	analytic model $BZ=BZ(X)$ at $Z = 4$ mm (T)
0	0.194893187
0.5	0.19286722
1	0.186912279
1.5	0.177400819
2	0.164952554
2.5	0.150397003
3	0.13468007
3.5	0.118728154
4	0.103316946
4.5	0.088993034
5	0.076064351
5.5	0.064641129
6	0.054696562
6.5	0.046123712
7	0.038778275
7.5	0.032506214
8	0.027159441
8.5	0.022603437
9	0.018720007
9.5	0.015407361
10	0.012578875
10.5	0.01016134
11	0.008093098
11.5	0.006322283
12	0.0048052561
12.5	0.003505
13	0.002391
13.5	0.001437
14	0.000620
14.5	-0.000078
15	-0.000674
average of analytic $BZ$ from $X = 0$ to $4$ mm	
0.158238692	
Approximation: $BZ \text{ max} * 0.8$	
0.15591455	
absolut error (Tesla)	
-0.002324143	
%	
1.47	

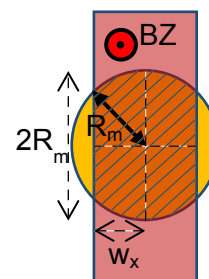
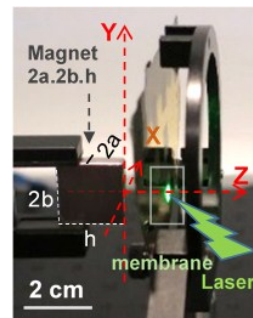


**Table1.** Magnetic field  $BZ(X)$  for the given  $Z = 4$  mm (Independently, membrane radius  $R_m = 4$  mm).